The precipitation mechanisms of typhoon Nari (2001) revealed by the Doppler radars, ISS and disdrometer observation

Tai-Chi Chen Wang, Wei-Yu Chang, Wei Tsung Lin, Shin-Hung Lin
National Central University
Jen-Hsin Teng
Central Weather Bureau

1. Introduction

About typhoon Nari(2001), Sui et. al. (2002) had provided a nice review of it's general characteristics. The radar data sets collected from WSR88D at Wufensan and CAA at CKS airport were edited and synthesized through RASTA (2000), a terrain following Doppler wind synthesis program. The three dimensional thermodynamic field at different stages during Nari's landfall were retrieved by the method developed by Liou et al.(2003) The 2-D video disdrometer provided detail drop size distribution during landfall. Together with the ISS (Integrated Sounding System) profiler data, very interesting contrast were found in the microphysical structure.

2. The maintenance of the pressure deficit after landfall

The dual Doppler synthesis wind fields at three time periods, 1600, 1630 UTC at Sep 16 and 0200 UTC at Sep 17 were derived. Fig.1 showed the wind field and isotach at 1600 UTC. The vortex center of Nari still could be clearly identified two hours after landfall. We found the wind was still quite circular, however the 20m/sec isotach banded along the terrain, indicating the blocking of terrain forced the strong wind to blow around the terrain and converge with the weaker wind at outer skirt at lower level to form a rainband. This rainband moved slowly toward northwest and brought heavy rain to Taipei. Although the maximum wind radius expanded to 40km in the NW-SE direction, and 20 km in the NE-SW direction, the relative pressure deficit still could be maintained. (Fig.2) The warm core about 4 degree was found in the circulation center. (Fig.2 and Fig.3) The vertical pressure gradient force and warming near the center are responsible for the maintenance of the weaken typhoon. The results from both the terrain following synthesis and the three dimensional variation retrieval of perturbation pressure provided much deeper insight of the thermodynamic structure of a landing typhoon. It proved that even the tangential circulation was decreased after landing, because of the low pressure was maintained, the slow moving typhoon system still can draw the moist air from surrounding ocean and provide fuel to the convection to keep the core warm and the depression of pressure.

3. The Drop Size Distribution and rainfall characteristics

In Nari case we have analyzed 12hrs data of disdrometer, the detail of the results of the heaviest rain period were shown. A quality control sequence was applied to the raw disdrometer data; the vertical velocity of the drops with unreasonable fall velocity and oblateness was changed to the empirical fall speed formula. The Gamma distribution of the Drop Size distribution were calculated by moment method. The analysis of N0 , m , Λ indicated the smaller m , Λ are associated with larger rainfall rate. In the same time, the smaller Λ was associated with the heavier

rainfall rate, and greater b associated with the lighter rainfall rate. In the statistics of these parameters in 12 hours, the coefficient m , Λ , b and A had the same tendency. During the heaviest rain, the drop size maximum was about 5mm. The increased rainfall rate is mainly due to the increase of the number of drops in Nari's case.

Between the ISS observation, 0200-0230 (Fig.4) we found the vertical motion are quite uniform structure in heavy rain period. On the contract 1300-1330, much bigger but much less raindrops were found in lighter rain. The vertical motion also has wider range, indicating a different type of rain drop size distribution, one day after landing.

4. summary

The disdrometer, Integrated Sounding System, rain gauge network and dual-Doppler radar data were collected during Nari's landfall. The terrain following dual Doppler synthesis wind field showed the structure change of circulation and the topographic influence. It explained the location and duration of the heavy rain after the landfall. From the thermodynamic retrieval results, the persistent circulation of Nari after landing maintained the low pressure center, the mean radial convergence at low level provided the moisture need of the convection. The terrain blocking decided the location of rainband, which was responsible for the heavy rain in the basin area. During the heaviest rain fall period, the disdrometer derived DSD indicated the upper limit of the drop size was about 5mm (Fig.4, Fig.7, Table.1), the number of drops increased very fast and dumped heavy rainfall. From the dual Doppler synthesis, the localized horizontal convergence of the drops may explain the torrential rainfall rate. The profiler observation of ISS(Integrated sounding system) enhance the microphysical understanding in the vertical direction. Through the synthesis of radars, profiler, disdrometer and raingauge network data, the unique three dimensional structure of typhoon Nari and possible precipitation mechanisms were partially revealed.

Reference:

Teng, J.-H., C.-S. Chen, T. C. Wang, and Y.-L. Chen, 2000: Orographic effects on a squall line system over Taiwan., *Mon. Wea. Rev.*, 128, 1123-1138.

Sui, C.-H., C.-Y. Huang, Y.-B. Tsai, C.-S. Chen, Pay-Liam Lin, S.-L. Shieh, M.-H. Li, Y.-A. Liou, T.-C. Chen Wang, R.-S. Wu, G.-R. Liu, Y.-H. Chu et al, 2002: Typhoon Nari and Taipei Flood- A Pilot meteorology-hydrology Study. Submitted to EOS, Transcations.

Liou Y.-C. , T.-C. Chen Wang, K.-S. Chung 2003: A Three-Dimensional Variational Approach for Deriving the Thermodynamic Structure Using Doppler Wind Observations – An Application to a Subtropical Squall Line., J. Applied Meteorology.,

Acknowledgement

This research is sponsored by the National Science council of Taiwan, ROC, under NSC 91-2119-M-002-032

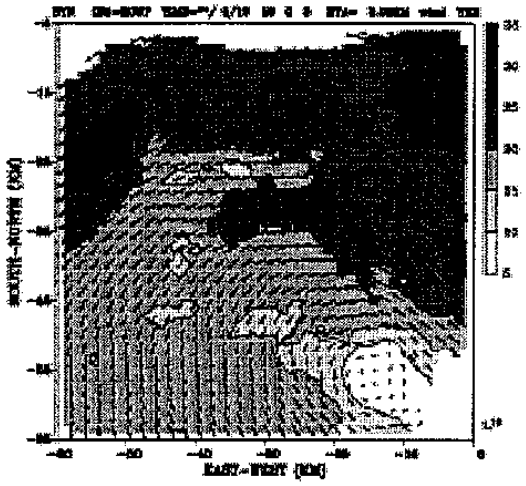

Fig1. Wind and isotach at 3km above terrain on Sep. 16 1600Z.

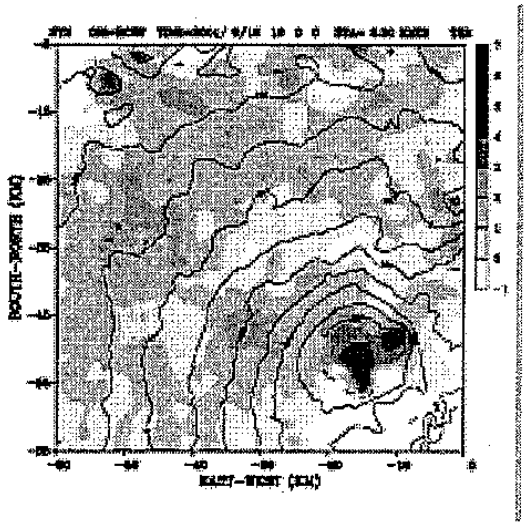

Fig2. Same as Fig.1 except for pressure and buoyancy perturbation.

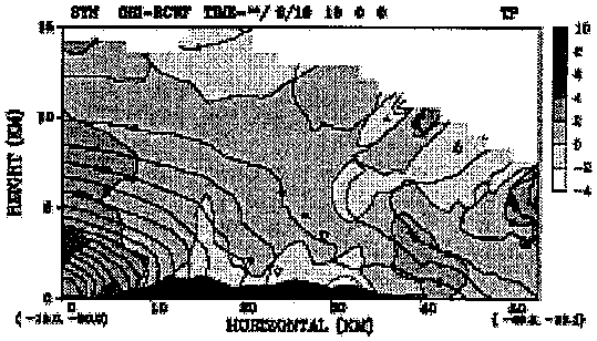

Fig3. The cross-section of pressure and buoyancy perturbation through (-15, -50) and (-50, -10) in Fig.1.

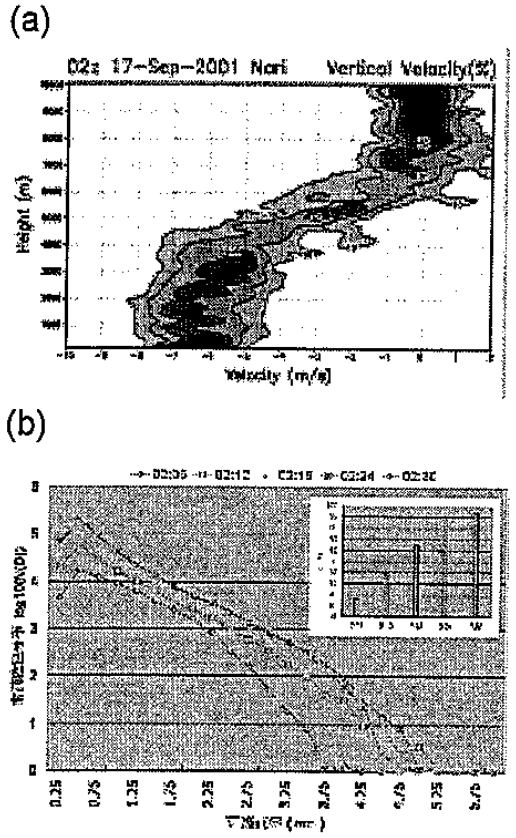

Fig4. (a) The frequency percentage of vertical motion from Sep. 16 0200 to 0230 (UTC).
(b) The drop size distributions.

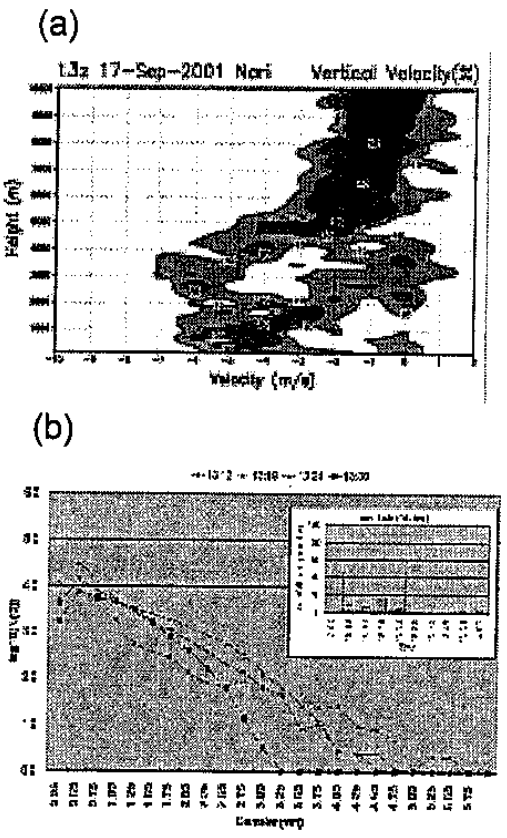

Fig5. Same as Fig 4. (a) (b) except from Sep.17 1300 to 1330(UTC).

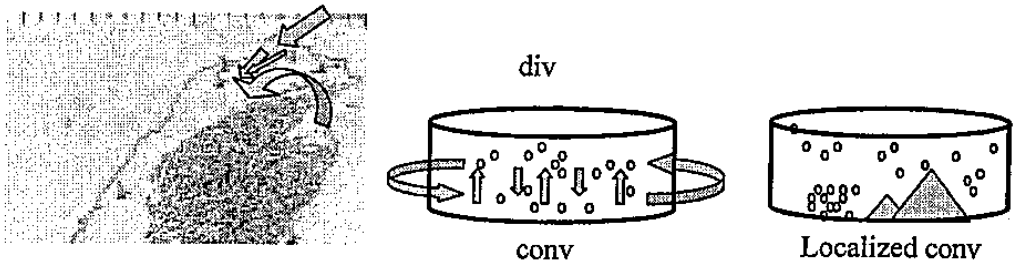

Fig6. Conceptual model of rainfall distribution during Nari's landfall.

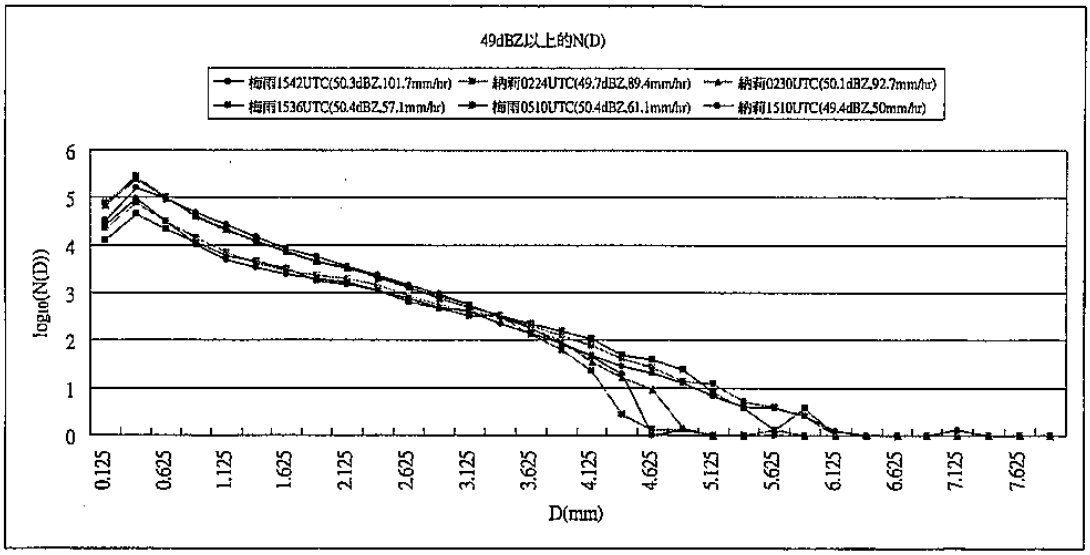

Fig7. The dropsize distribution of torrential rain and heavy rain cases

	事件	dBZ	R(mm/hr)	m	Λ	N0	A	b	D0(mm)	D0r(mm)
	梅雨 (2001.05.09)1542UTC	50.441	101.063	0.9	2.5698	4.63E+04	158.8	1.4183	1.778	1.625
A	納莉 (2001.09.17)0224UTC	49.72	87.789	0.69	2.5097	4.06E+04	152.6	1.4346	1.738	1.625
	納莉 (2001.09.17)0230UTC	50.22	92.06	0.48	2.3522	3.49E+04	147.8	1.4522	1.765	1.625
	梅雨 (2001.05.09)1536UTC	50.82	58.256	1.39	2.1057	5.61E-05	45.53	1.8345	2.401	2.375
B	梅雨 (2001.05.09)0510UTC	50.67	61.963	1.28	2.181	7.70E-05	49.31	1.8071	2.374	2.125
	納莉 (2001.09.17)1510UTC	49.89	50.254	0.606	1.9287	6.05E-05	40.11	1.8417	2.228	2.125

Table1. The GAMMA distribution parameters and Z-R relations in torrential rain and heavy rain cases